Special Issue
"Progress of Theoretical and Computational Biophysics"

Vol. 16, pp. 220–231 (2019)
doi: 10.2142/biophysico.16.0_220

Biophysics and Physicobiology

https://www.jstage.jst.go.jp/browse/biophysico/

Regular Article

Dynamic properties of oligomers that characterize low-frequency normal modes

Hiroshi Wako[1] and Shigeru Endo[2]

[1]*School of Social Sciences, Waseda University, Shinjuku-ku, Tokyo 169-8050, Japan*
[2]*Department of Physics, School of Science, Kitasato University, Sagamihara, Kanagawa 252-0373, Japan*

Received May 27, 2019; accepted July 9, 2019

Dynamics of oligomeric proteins (one trimer, two tetramers, and one hexamer) were studied by elastic network model-based normal mode analysis to characterize their large-scale concerted motions. First, the oligomer motions were simplified by considering rigid-body motions of individual subunits. The subunit motions were resolved into three components in a cylindrical coordinate system: radial, tangential, and axial ones. Single component is dominant in certain normal modes. However, more than one component is mixed in others. The subunits move symmetrically in certain normal modes and as a standing wave with several wave nodes in others. Secondly, special attention was paid to atoms on inter-subunit interfaces. Their displacement vectors were decomposed into intra-subunit deformative (internal) and rigid-body (external) motions in individual subunits. The fact that most of the cosines of the internal and external motion vectors were negative for the atoms on the inter-subunit interfaces, indicated their opposing movements. Finally, a structural network of residues defined for each normal mode was investigated; the network was constructed by connecting two residues in contact and moving coherently. The centrality measure "betweenness" of each residue was calculated for the networks. Several residues with significantly high betweenness were observed on the inter-subunit interfaces. The results indicate that these residues are responsible for oligomer dynamics. It was also observed that amino acid residues with significantly high betweenness were more conservative. This supports that the betweenness is an effective characteristic for identifying an important residue in protein dynamics.

Key words: betweenness, degeneracy of normal modes, conservation of amino acid residues, protein structure network, cylindrical coordinate system

Most proteins function in an oligomeric form [1]. An advantage of oligomers over monomers is that the oligomeric form permits proteins to initiate allostery and cooperativity in achieving their function. Studies on the dynamics of oligomers can provide key information that reveals the mechanism of the allostery and cooperativity. Molecular dynamics (MD) simulation and normal mode analysis (NMA) can be effective theoretical methods to address this problem [2–9]. Although they can generate a large amount of data regarding protein motions at the atomic level and the motions

Corresponding author: Hiroshi Wako, School of Social Sciences, Waseda University, 1-6-1 Nishi-Waseda, Shinjuku-ku, Tokyo 169-8050, Japan.
e-mail: wako@waseda.jp

◀ ***Significance*** ▶

Dynamics of oligomeric proteins were studied by elastic network model-based normal mode analysis to characterize their large-scale concerted motions. (1) The rigid-body motions of individual subunits were characterized by the radial, tangential, and axial components in a cylindrical coordinate system. (2) The motions of atoms on the inter-subunit interfaces were characterized by the opposing motions of intra-subunit deformation and rigid-body motion of the subunit. (3) A dynamic protein structure network was defined in each mode, and the centrality measure, betweenness, was calculated for each residue. The results indicate that the residues with high betweenness play an important role in oligomer dynamics.

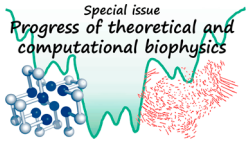

are observable on a computer monitor through animation, it is not convenient to extract significant and comprehensive information from them and understand oligomer dynamics.

In this study, we examined several properties associated with oligomer dynamics. These could be determined by NMA calculation and may be effective for characterizing the dynamics. We used an elastic network model-based NMA program developed by us, called PDBETA [10,11]. This has been developed based on the previous NMA program, FEDER/2 [12]. In that program, the regular conformational energy functions based on the molecular mechanics are integrated, and conformational energy minimization is required prior to the application of NMA.

The programs, FEDER/2 and PDBETA, are different from other similar programs with respect to the independent variables used in the NMA calculation. That is, they use dihedral angles around rotatable chemical bonds, whereas most other programs use Cartesian coordinates. The computational algorithms for a dihedral angle system were developed and advanced by Professor Gō's group [13–16]. Initially, it was applicable only to a monomer system. However, it was extended to an oligomer in an effective and convenient formulation. Consequently, their availability has been broadened significantly [17]. They were applied to hemoglobin by Seno and Gō in 1990 [2,3] and came to fruition in FEDER/2.

Out of the various properties calculated by PDBETA [11,18], we focused on the displacement vectors of individual atoms in the ten lowest-frequency normal modes, in this study. Most researches of NMA were interested in time-averaged properties. These are calculated by averaging certain specific properties such as atomic fluctuations and the cross-correlations between them, over all the normal modes. However, we confined ourselves to characterizing the motions of individual lowest-frequency normal modes because there are many studies that elucidate their key features associated with their protein functions [19–22].

First, we considered simplifying the oligomer motions for a comprehensive understanding. That is, rigid-body translational and rotational motions of the subunits were determined from individual sets of displacement vectors of their constituent atoms. Because homo-oligomers are frequently arranged in a ring structure, it would be convenient if these motions are decomposed into their radial, tangential, and axial components in a cylindrical coordinate system. This decomposition made it convenient for us to image the individual subunit motions.

Secondly, the motions of residues on the inter-subunit interfaces were examined. We were interested in the relationship between the motions of the entire oligomer and those of the individual subunits. In particular, we were interested in the outcome of an increase in the number of subunits. It was already demonstrated that the oligomers (hexamer [7], trimer [8], 12 mer [9], and 13 mer [9]) extensively exploited the dynamic features of the individual subunits. We verified this focusing on the difference between the motions of inter-subunit interface residues and those of non-interface ones.

Finally, protein structure network (PSN) analysis was applied to predict important residues on the inter-subunit interfaces. In this study, the PSN was defined for individual normal modes and is thus referred to as a dynamic PSN. A PSN defined based on the PDB structure is referred to as a static PSN. The dynamic PSN consisted of a node and an edge. A residue was treated as the node, and the edge was defined as a link between two residues that made contact with each other and moved coherently in a specific normal mode. A residue centrality in the network such as closeness and betweenness is generally used to predict important residues for transmitting information across a protein structure [23–30]. We paid special attention to two residues with high betweenness linked in the dynamic PSN and located on different subunits. They were considered to play a potentially important role in oligomer dynamics.

These analyses have presented a new approach to image the oligomer dynamics and may help to identify potentially important residues in the oligomer dynamics.

Materials and Methods

Proteins examined

Oligomer PDB data with a resolution less than 1 Å and requiring moderate calculation were selected. Four trimers, eight tetramers, and three hexamers were identified. There was no pentamer. In this paper, we discuss the following four homo-oligomers: Cu nitrite reductase from *Achromobacter cycloclastes* (trimer; PDB ID: 5akr [31]; abbreviated as AcNiR; 378×3=1,134 amino acid residues), L-asparaginase from *Erwinia chrysanthemi* (tetramer; 1o7j [32]; ErA; 327×4=1,308 a.a.), benzoylformate decarboxylase (tetramer; 2fn3, Bera, A. K. & Hasson, M. S., unpublished data; BFD; 528×4=2,112 a.a.), and uridine phosphorylase from *Shewanella oneidensis* (hexamer; 4r2x [33]; SoUP; 252×6=1,512 a.a.). Whereas the PDB data 1o7j and 4r2x include atomic coordinate data of the whole oligomers, 2fn3 and 5akr do not. The atomic coordinate data in an oligomeric state were obtained from PDBj for 2fn3 and 5akr.

Their 3D structures are shown in Figure 1. The subunits of AcNiR, BFD, and SoUP are arranged in a ring form, whereas those of ErA are in a closed-packed (or dihedral) form. In BFD, the neighboring subunits are flipped upside-down from each other. SoUP can be regarded as a trimer of homodimers.

Normal mode analysis of oligomers

Elastic network model based NMA was applied to oligomeric proteins using a computer program we have developed [11]. All the atoms in the PDB data were considered in the computations. Out of the various properties calculated in that program, we focused on the displacement vectors of individual atoms, $\Delta r_{\alpha\lambda}$, in the ten lowest-frequency normal modes, as described in Introduction. The suffixes α and λ

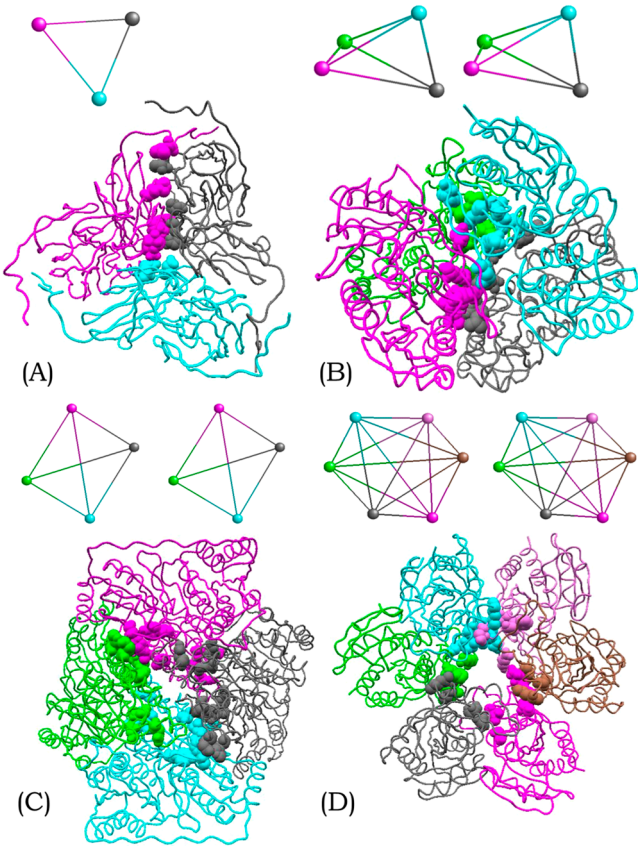

Figure 1 3D structures of proteins examined in this study. (A) Cu nitrite reductase (trimer; AcNiR; PDB ID: 5akr), (B) L-asparaginase (tetramer; ErA; 1o7j), (C) benzoylformate decarboxylase (tetramer; BFD; 2fn3), and (D) uridine phosphorylase (hexamer; SoUP; 4r2x). Chains A, B, C, D, E, and F are colored grey, magenta, cyan, green, brown, and violet, respectively. The residues shown in a space-filling model are located on the inter-subunit interface and have higher BTWN (see Fig. 7). The solid figures in a stereo view above individual 3D structures show the spatial arrangements of the constituent subunits represented by colored balls. Their point groups are (A) C_3, (B) D_2, (C) D_2, and (D) D_3.

indicate an atom and normal mode number, respectively.

The displacement vector, $\Delta r_{\alpha,\lambda}$, calculated for the whole oligomer can be decomposed into two vectors for each subunit: an intra-subunit deformative motion (internal motion), $\Delta r^{\mathrm{int}}_{\alpha,\lambda}(k)$, and a rigid-body motion of a subunit (external motion), $\Delta r^{\mathrm{ext}}_{\alpha,\lambda}(k)$ [5,8]. The displacement vector, $\Delta r_{\alpha,\lambda}$, contains no contribution from the external degrees of freedom for the whole oligomer. This is because the set of displacement vectors for the whole oligomer are calculated so as to satisfy the Eckart condition. Meanwhile, a set of the displacement vectors, $\Delta r^{\mathrm{int}}_{\alpha,\lambda}(k)$, of atoms α in subunit k is determined so that it satisfies the Eckart condition with respect to only subunit k. The external motion vector, $\Delta r^{\mathrm{ext}}_{\alpha,\lambda}(k)$, is defined as the difference between $\Delta r_{\alpha,\lambda}$ and $\Delta r^{\mathrm{int}}_{\alpha,\lambda}(k)$, i.e., $\Delta r^{\mathrm{ext}}_{\alpha,\lambda}(k) = \Delta r_{\alpha,\lambda} - \Delta r^{\mathrm{int}}_{\alpha,\lambda}(k)$. The external motion is a rigid-body motion of subunit k (see [8] for further details).

The translational and rotational vectors for the rigid-body motion of the λth normal mode of subunit k are defined as follows using $\Delta r^{\mathrm{ext}}_{\alpha,\lambda}(k)$ [8]:

$$T_{k,\lambda} = \frac{\sum_\alpha m_\alpha \Delta r^{\mathrm{ext}}_{\alpha,\lambda}(k)}{\sum_\alpha m_\alpha},$$

$$R_{k,\lambda} = \Gamma_k^{-1} \sum_\alpha m_\alpha (r_\alpha^0 - r_k^G) \times \Delta r^{\mathrm{ext}}_{\alpha,\lambda}(k),$$

where m_α is the mass of the atom α; r_α^0 and r_k^G are the coordinate vectors of atom α in the PDB conformation and the center of mass of subunit k, respectively; and Γ_k is an inertia tensor of subunit k. The summation is carried out over the atoms in subunit k. The measurement units of the two vectors, $T_{k,\lambda}$ and $R_{k,\lambda}$, are Å and radians, respectively.

Cylindrical coordinate system

In order to comprehensively image the translational and rotational motions of the subunits defined above, we considered representing the two vectors, $T_{k,\lambda}$ and $R_{k,\lambda}$, in the cylindrical coordinate system defined in individual subunits. The cylindrical coordinate system of a subunit was defined as follows (Fig. 2).

First, the Z-axis is defined for the whole oligomer. The origin is set to the center of mass of the oligomer. Then, the principal axes are calculated from the inertia matrix for the oligomer. The principal axis corresponding to the largest principal moment of inertia is defined as the Z-axis. The positive direction of the Z-axis can be determined arbitrarily. The Z-axis corresponds to a rotation axis of the oligomer in a ring form (AcNiR, BFD, and SoUP in this study). For the oligomer in a close-packed form (ErA in this study), the Z-axis is one of its symmetry axes.

Next, for a specific subunit, the origin is set to its center of mass. The z-axis of the subunit is defined as a line passing through the center of mass of the subunit and parallel to the Z-axis of the oligomer. A radial axis is a perpendicular dropped from the center of mass of the subunit to the Z-axis of the oligomer. The positive radial axis is directed radially away from the Z-axis of the oligomer. Finally, a tangential axis is defined by a cross product of two unit vectors parallel to the z- and radial axes, respectively.

Then, unit vectors with similar directions as the translational and rotational vectors, $T_{k,\lambda}$ and $R_{k,\lambda}$, calculated for individual subunits were decomposed into their respective three components: radial, tangential, and z-axis ones. The motions represented by these components of the translational and rotational vectors are depicted in Figure 2.

Interface residues between subunits

We considered the difference between the residues on the inter-subunit interfaces (interface residues) and the other residues. The latter could be either in the subunit interior or on the surface exposed to the solvent (non-interface residues). The interface and non-interface residues were defined as follows. First, the accessible surface area (ASA) of each

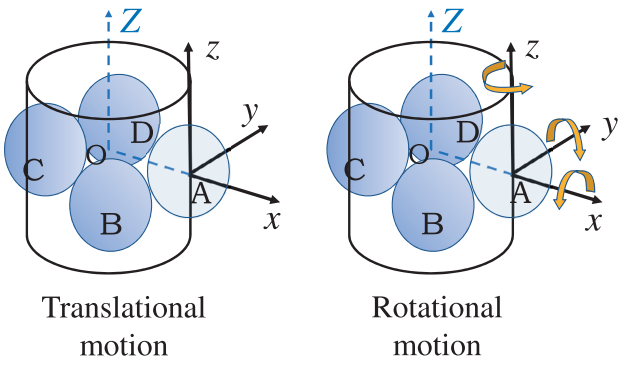

Figure 2 The cylindrical coordinate system defined in each subunit. The three axes, *x*, *y*, and z, indicate the radial, tangential, and z-axes. The Z-axis is a symmetry axis of the oligomer. A tetramer composed of subunits A, B, C, and D in a ring form is illustrated. In the translational motions, the arrows of the axes directly indicate the directions of translational motions. In the rotational motions, the arrows of the axes indicate the rotation axes around which the subunit rotates as shown by the orange rotation arrows.

residue was calculated separately for an oligomer state and isolated monomer state. Then, if the ASAs of a specific residue for the two states differed, this residue was regarded as an interface residue. Otherwise, it was defined as a non-interface residue.

Betweenness

Recently, a network analysis based on graph theory, which is popular in social sciences and complex-system studies, has been applied to a protein structure to elucidate structurally and functionally important residues, intra- and inter-protein communication, and allostery [23–30]. The network analysis is considered to be effective for revealing the communication between remote residues via other residues in the protein.

In this study, the protein structure network (PSN) was defined individually for the ten lowest-frequency normal modes, in addition to the static structure. The network is composed of vertices and edges. A Cβ atom is assigned to a vertex for representing a residue (a Cα atom for a Gly residue). For the network based on the PDB structure (static PSN), spatially neighboring residues were connected by an edge. That is, if at least one atom from a residue is closer than a specified cutoff distance (5.0 Å in this study) to at least one atom from another residue, these two residues were connected by an edge. For the network based on the normal mode motion (dynamic PSN), two residues were connected by an edge if they were spatially neighboring and moved in a coherent manner. That is, an additional condition that the cosine of the displacement vectors of two Cβ atoms should be higher than a specified cutoff value (0.8 in this study) was added to the definition of the static PSN. This condition implies that the two connected Cβ atoms move in the same direction. The dynamic PSNs are subgraphs of the static PSN.

We calculated the betweenness centrality (BTWN) for each residue in these networks. For each pair of residues in a network, a shortest path between them exists. The BTWN for a residue *x* is defined as the number of these paths that pass through the residue *x*. Typically, there is more than one shortest path for a specific pair. The standard extension of BTWN to this case assigns each path a weight equal to the inverse of the number of paths. Accordingly, BTWN of vertex *x* is defined as

$$\mathrm{BTWN}(x) = \frac{2}{(n-1)(n-2)} \frac{1}{2} \sum_{s,t} \frac{\eta_{st}(x)}{\eta_{st}},$$

where η_{st} is the number of shortest paths from vertex *s* to vertex *t*, and $\eta_{st}(x)$ is the number of shortest paths from vertex *s* to vertex *t* that pass through vertex *x*; *n* is the total number of vertices, and $(n-1)(n-2)/2$ is a normalization factor.

A residue with higher BTWN would have more control over the network because more residues communicate with each other passing through that residue.

Residue conservation

The evolutionary conservation of residues in an amino acid sequence was examined in relation to the BTWN. The close relationships between sequence conservation and dynamics have been discussed for several proteins [34–36]. We obtained residue conservation data for PDB data at ConSurf-DB [37] through PDBsum [38]. The evolutionary conservation of each amino acid position was calculated based on multiple sequence alignment in this database. However, the data for only two of the four proteins examined in this study, 1o7j and 2fn3, were available in this database.

Results

Motions represented in the cylindrical coordinate system

Oligomer motions are generally represented by the displacement vectors of the constituent atoms. Although they can provide sufficient information on the oligomer motions, it is too complex to be learnt comprehensively. It may be effective to simplify the oligomer structure for understanding them. For this purpose, we regarded individual subunits as rigid bodies and examined their translational and rotational motions.

For the convenience of describing the various motions of an oligomer, we introduce a shorthand notation for a subunit motion. It is indexed with three elements: (1) a translational or rotational motion (TL or RT), (2) its components in the cylindrical coordinate system (CCS), i.e., radial, tangential, and z-axis ones (r, t, and z), and (3) normal mode number (from one to 10). Therefore, we refer to, for example, a radial component of a translational vector in mode 1 and a z-axis component of a rotational vector in mode 5 as TL-r-1 and RT-z-5, respectively.

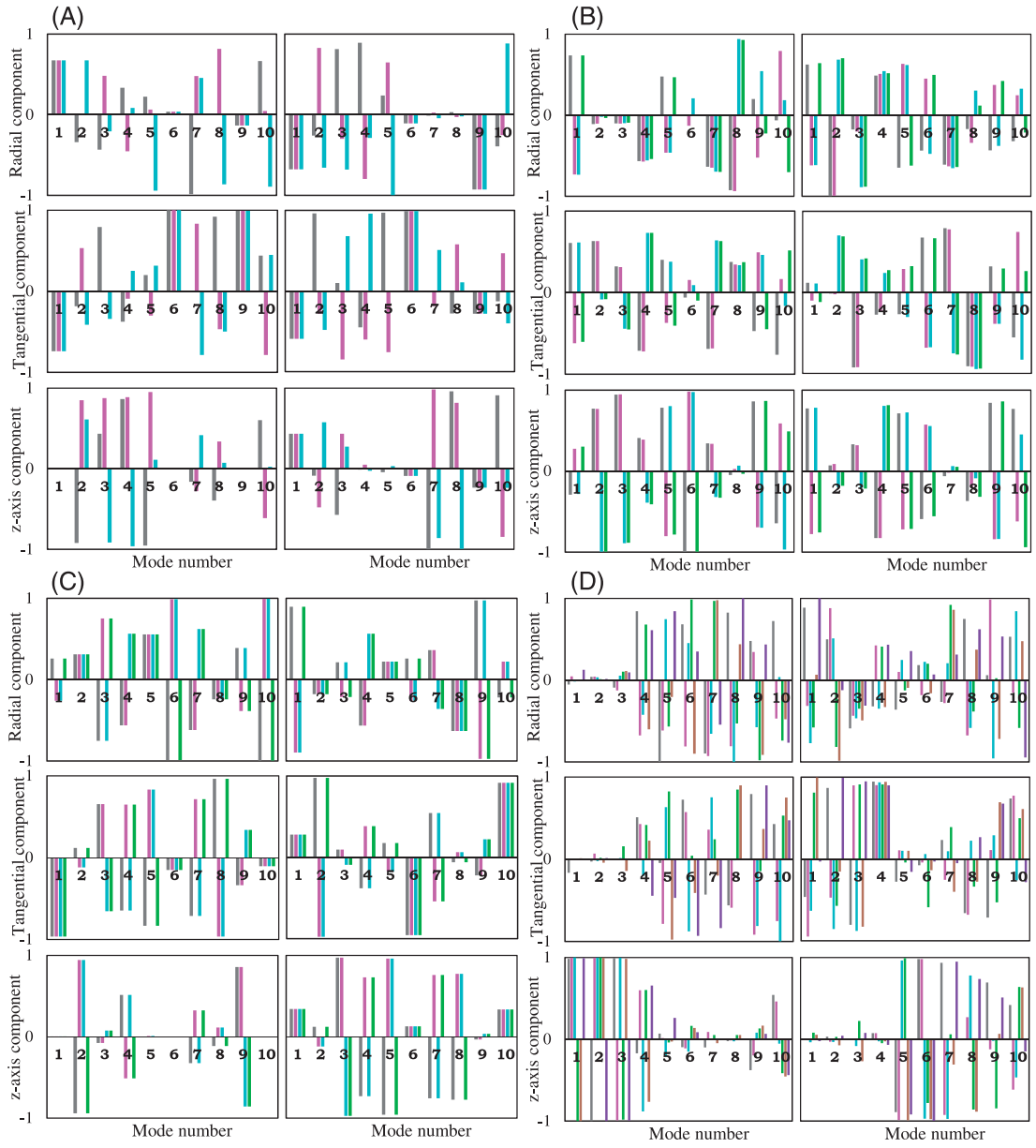

Figure 3 Subunit motions in the cylindrical coordinate system. The cylindrical components (radial, tangential, and z-axis ones) of the translational and rotational motions of subunits for the ten lowest-frequency normal modes are shown for four oligomers; (A) AcNiR, (B) ErA, (C) BFD, and (D) SoUP. For each oligomer, three panels from top to bottom in the left and right columns show the radial, tangential, and z-axis components, respectively. The left and right columns are for the translational and rotational motions, respectively. In a panel, a set of bars (3, 4, 4, and 6 bars in (A)–(D), respectively) shows the components of the individual subunits for a specified normal mode.

Figure 3 shows the magnitudes of the CCS components of the constituent subunits of an oligomer. The three panels on the left are for the translational motion, and those on the right for the rotational motion. From top to bottom, the radial, tangential, and z-axis components are shown. Each panel shows these components of the constituent subunits for ten normal modes. Because they are components of unit vectors with similar directions as the translational and rotational vectors, respectively, their absolute values are less than or equal to one.

In Supplementary Figure S1, the motions of oligomers are depicted with respect to subunit motions for several normal modes.

We observed two major types of motions of the oligomer: a symmetric type and a standing-wave type. In a symmetric-type motion, all the subunits have CCS components of nearly equal magnitude. This implies that they undergo identical motion. Meanwhile, in a standing-wave-type motion, the magnitudes of the CCS components differ depending on the subunits. This type of motions can be classified further

according to the number of waves, *m*, including the case where two or more waves with different *m* are superposed. In the standing-wave-type motion, the subunits vibrate similarly albeit with phase differences among themselves.

In the symmetric-type motion, if all the radial components of a translational motion are identical, the oligomer exhibits a symmetric stretching/shrinking motion in the radial direction. This is observed in TL-r-1 of AcNiR, TL-r-4 and 7 of ErA, and TL-r-5 of BFD. If all the tangential components are identical, the oligomer exhibits a rotational vibration around the z-axis. This is observed in TL-t-1, 6, and 9 of AcNiR, and TL-t-1 of BFD. If all the z-axis components are identical, the entire oligomer vibrates along the z-axis. It is not permitted in NMA because such a motion does not satisfy the Eckert condition. Such a motion is not observed.

With regard to the rotational motion of a subunit, if all the radial components are identical, all the subunits are rotated around the radial axis in a similar direction. This is observed in RT-r-4 and 7 of ErA, RT-r-8 of BFD, and RT-r-1 and 9 of SoUP. If all the tangential components are identical, the oligomer is in a rolling mode. Herein, residues on a surface move to the center, and those on the opposite surface move away from the center. This is observed in RT-t-1 and 6 of AcNiR, RT-t-8 of ErA, RT-t-6 and 10 of BFD, and RT-t-4 of SoUP. If all the z-axis components are identical, all the subunits are rotated around the z-axis in a similar direction. This is not observed in this study (although RT-z-1 in AcNiR and RT-z-1, 6, and 10 of BFD are of this type, their magnitudes are too small to be significant, compared to the other components).

The standing-wave-type motions can be classified according to the number of waves, *m*. For example, in the radial components of a translational motion of BFD, m=1 for TL-r-6 and 10, and m=2 for TL-r-3. For a tetramer and a hexamer, m=2 and 3, respectively, indicate that the motions of neighboring subunits are similar albeit in the opposite direction (i.e., phase shift is π). Comparatively, for a trimer AcNiR, it is not feasible to move in a similar manner.

The superposition of more than one wave is also observed. For example, in the hexamer SoUP, the superposition of the waves of m=0 and 1 is observed in RT-r-7; m=0 and 3 in RT-t-10; m=1 and 3 in RT-r-9; and m=1 and 2 in TL-r-4, TL-t-5, TL-z-1, and RT-z-7.

The degeneracy of eigenvalues occurred in AcNiR. They are mode pairs, 2 and 3, 4 and 5, and 7 and 8. The mode pairs show similar motion patterns, with shifted phases. The pair of neighboring modes with considerably close frequencies was also determined: modes 2 and 3 in ErA, 7 and 8 in BFD, and 5 and 6 in SoUP. They too exhibit similar motion patterns with phase shifts from each other.

In certain normal modes, a component is dominant over the others, whereas in others, more than one component is mixed. For example, the motions are represented essentially by one component in the following modes: TL-t-6 and 9, TL-z-4, RT-r-4, and RT-t-6 in AcNiR; TL-z-6 and RT-t-8 in ErA; TL-r-6, TL-t-1, TL-z-2, RT-r-1 and 9, RT-t-2, 6, and 10, and RT-z-3 and 5 in BFD; and TL-z-1 to 3 and RT-z-5 to 7 in SoUP. In most of the remaining modes, two components are mixed.

These results reveal that there are a variety of oligomer motions depending on the normal modes. Moreover, the representation in the cylindrical coordinate system is a comprehensive approach to imaging the motions.

Interface residues between subunits

A noteworthy question regarding oligomer dynamics is how much of the intrinsic dynamics of each subunit is maintained. Is it more effective to regard an oligomer as an elastic continuum body as the number of subunits increases? To answer this, several studies were carried out. They demonstrated that the oligomer exploited the intrinsic dynamics of the constituent subunits. We validated it from a different perspective.

Figure 4 shows the frequency distributions of the cosine of the internal and external displacement vectors for the inter-subunit interface and non-interface residues for BFD. The data for AcNiR, ErA, and SoUP are not presented here because they exhibit patterns similar to that of BFD. The distributions in the two panels differ distinctively. The cosines of most residues on the inter-subunit interface (Fig. 4A) are negative and close to -1. Meanwhile, they are distributed more uniformly for the non-interface residues (Fig. 4B). This biased distribution of the interface residues indicates that the internal motion (i.e., intra-subunit deformative

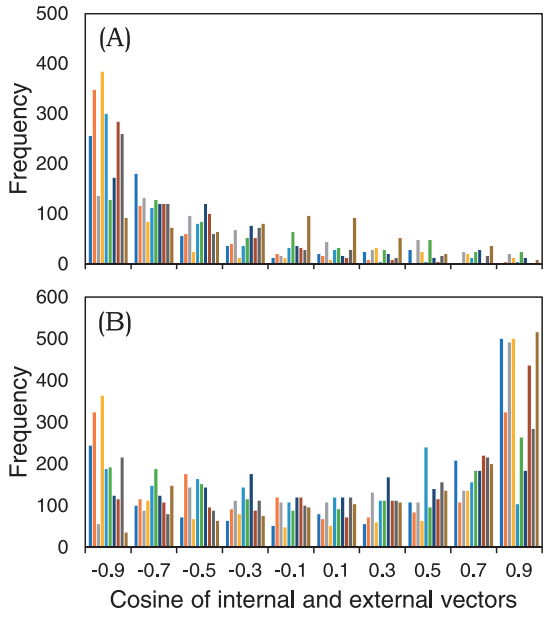

Figure 4 Frequency distributions of cosine of internal and external displacement vectors for (A) inter-subunit-interface and (B) non-interface residues for BFD. A set of ten bars in each bin (width of 0.2) shows the frequencies for the first to tenth normal modes (from left to right) with different colors.

motion) of the interface residues is in the opposite direction with respect to that of the external motion (i.e., rigid-body motion) of the subunit. Consequently, the two motions are cancelled out to preserve the native conformation. Meanwhile, the uniform distribution of the non-interface residues implies that they fluctuate under the intrinsic dynamics of individual subunits, independently of the rigid-body motions of the subunits.

The opposing motions between the external and internal motions were indicated for an interface between an enzyme protein and its inhibitor [5]. Then, it verified in dimers [39] and trimers [8]. In this study, they have been verified in other oligomers. In addition, they are observed to be commonly present in the motions of the lowest-frequency normal modes.

The distinctive difference between the motions of interface and non-interface residues indicates that it is not adequate to regard an oligomer as an elastic continuum body. Moreover, at the same time the motions of inter-subunit interface residues are strongly affected by the residues in the neighboring subunits.

Betweenness of residues

Figure 5 shows the BTWNs of residues for four oligomers. There are eleven BTWN profiles in each panel. The bottom profile shows the BTWN calculated for the PDB structure. Thus, this is a profile for the static PSN of the oligomer. The second-from-the-bottom to the top profiles show the BTWNs for the first to the tenth lowest-frequency normal modes, respectively. These are profiles for the dynamic PSNs defined for these normal modes individually. The residues specified in the PDB data as "SITE" are indicated with vertical lines. Although a few of them play a functional role and others mediate crystal packing contacts with small molecules, they are not distinguished in Figure 5. In the normal mode calculations, molecules bound to proteins (HETATM in PDB data) are excluded, except for thiamine thiazolone diphosphate in BFD. Active sites are also indicated if they are available from PDBj (residues 15, 29, 95, 96, 168, and 284 in ErA; and 28, 70, and 281 in BFD) [40].

In our experiences with BTWN calculations for many proteins, the residues with high BTWN are frequently observed around an active site, a binding site of small molecules, and a domain boundary. Because such specific residues do not necessarily have high BTWNs in all the normal modes, but usually in some of them, they can highlight the uniqueness of individual normal modes.

In Table 1, the binding site residues of small molecules and the active site residues with high BTWNs are listed. A few of the binding sites have high BTWN, indicating that many residues communicate with those sites in their fluctuations. It should be noted that the residues in the binding sites do not necessarily have high BTWN. That is, it may be feasible to predict dynamically important residues in the binding site according to their BTWN values.

The relationship between a domain boundary and BTWM is not evident in the oligomers examined here. The numbers of domains for AcNiR, ErA, BFD, and SoUP are one, two,

Table 1 Binding site and catalytic site residues with high BTWN [a)]

(A) AcNir		
Site identifier	Molecule	Residues
AC1	Cu	H145 (6), M150 (3, 9)
AC2	Cu	H100 (1, 2, 4, 10), H135 (1)
AC5	Malonate	F312 (4, 8), H319 (10)
AC6	Malonate	R250 (1, 5, 6, 8, 10), D251 (1, 3, 5, 6, 7, 8, 9, 10), R253 (2, 5, 6, 9), E310 (1, 6, 9, 10)
(B) ErA		
AC1	SO4	D96 (3, 6), K168 (4)
CC4	Glycerol	E181 (1, 2, 3, 4, 8, 10)
Catalytic site		D96 (3, 6), V284 (2, 4, 6, 7)
(C) BFD		
AC1	Magnesium	L118 (4), R120 (4, 6, 7)
AC5	TTDP [b)]	N23 (1), N77 (4, 5, 6, 7, 10), L403 (4, 6, 9), Y433 (6)
(D) SoUP		
AC1	SO4	R88 (3, 5, 7, 8, 9, 10), T91 (4)
AC2	Cl	Q163 (3), R165 (4)
AC3	Glycerol	E193 (3), M194 (7, 8, 9)
AC4	Glycerol	A204 (2, 7)
CC1	Glycerol	P122 (2, 3, 10), E124 (3, 7, 10)

a) The residues of the binding sites of small molecules and catalytic sites with BTWN>0.02 are listed. For the binding site, both the site identifier referred to in the PDB data and the molecule name are provided. In the parentheses after the residue name, normal mode numbers with BTWN>0.02 are shown.

b) TTDP: Thiamine thiazolone diphosphate

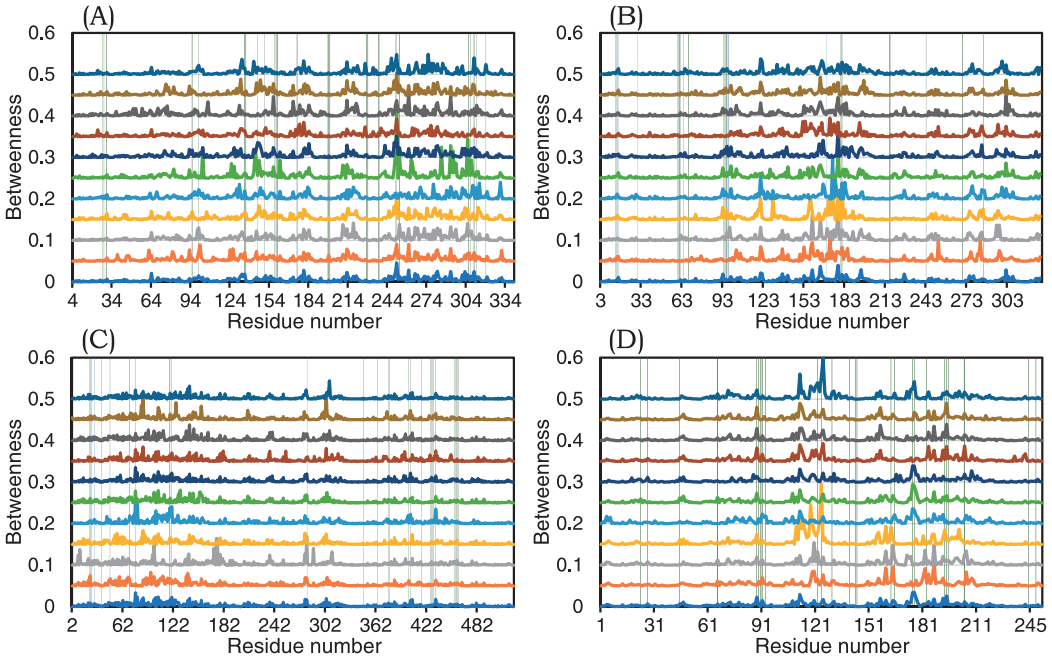

Figure 5 Betweenness of residues in PDB structure and ten lowest-frequency normal modes. (A) AcNiR, (B) ErA, (C) BFD, and (D) SoUP. The bottommost line is a BTWN profile for the static PSN, and the ten BTWN lines from the second-from-the-bottom to the top are BTWN profiles for the dynamic PSNs of the first to tenth normal modes, respectively. They are shifted upward by 0.05 successively from bottom to top for clarity. The vertical lines indicate residues specified in the PDB data as "SITE" and catalytic sites, if available.

three, and one, respectively. The domain boundary in ErA has a long linker, 207–219, and the BTWNs of the residues in the linker are very small. Meanwhile, BFD has two domain boundaries. One of them also has a long linker 329–354, and thus, the BTWNs of the residues in it are as small as the linker in ErA. In contrast, at another domain boundary, 179–180, residue 177 in mode 2 and residues 179 and 181 in mode 7 have high BTWN. This implies that these two modes are associated with the inter-domain motion.

Relationship between amino acid residue conservation and high BTWN

We were interested in whether or not amino acid residues with high BTWN are conservative. This was because amino acid residue conservation is a characteristic underlying their importance. In Figure 6, the conservation scores of residues are plotted against their BTWNs for ErA and BFD, whose amino acid conservation data were obtained from ConSurf-DB. The smaller is the conservation score, the more conservative is the residue. In the panels, the residues are classified into two groups: inter-subunit interface and

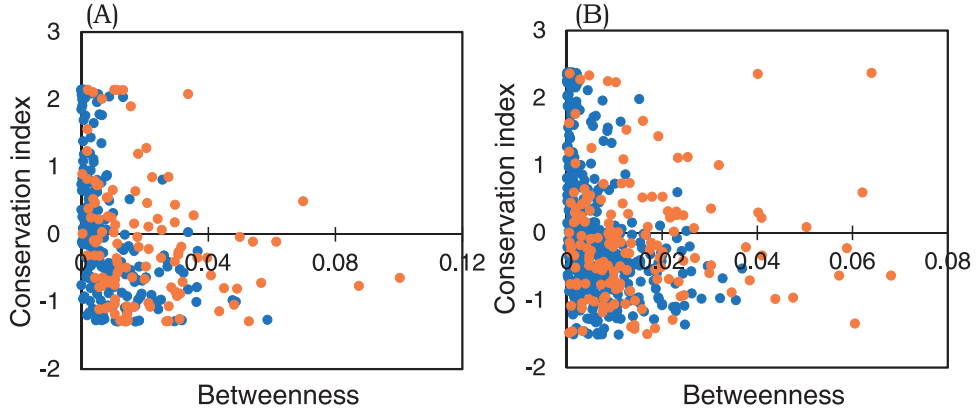

Figure 6 Correlation between conservation score (vertical axis) and BTWN (horizontal axis) of a residue. (A) ErA and (B) BFD. The colors orange and blue indicate inter-subunit interface and non-interface residues, respectively.

non-interface residues. More or less, the residues with higher BTWN are conservative and located on the inter-subunit interface. This implies that an amino acid residue with high BTWN is conservative and therefore, important in oligomer dynamics.

There are two peculiar residues with high BTWN that have low conservation scores in BFD. They are Gln170 and His173 [(betweenness, conservation score) = (0.040, 2.35) and (0.064, 2.37), respectively]. They are located on the inter-subunit interface and near the surface exposed to the solvent. They are also referred to in Figure 7C below. According to this figure, the two residues in one subunit are in contact with Tyr288 in another, which also has high BTWN. Meanwhile, the multiple sequence alignment of proteins homologous to this protein by ConSurf-DB illustrate that the region including Gln170 and His173 and another region including Tyr288 are highly diverse and that the corresponding residues are missing in a few proteins. It may imply that these regions are particularly adjusted for the dynamics of BFD within its homologous proteins.

Link between interface residues with high BTWN

The residues with high BTWN can be linked to each other to form an efficient and robust route for other residues to communicate among themselves. Figure 7 shows the residues on the inter-subunit interface that satisfy the following conditions: (i) the two residues linked by an edge are from different subunits, (ii) both of these have higher BTWNs than a specified value assigned to individual oligomers (0.05, 0.04, 0.04, and 0.04 for AcNiR, ErA, BFD, and SoUP, respectively; these values were determined arbitrarily; if smaller values were assigned, larger networks could be generated), (iii) they are in contact with each other (at least one atom from one residue is closer than 5.0 Å to at least one atom from another residue). These residues are also shown on the 3D structures in Figure 1. Because the network is constructed for individual normal modes, such a link between the residues is observed only in a few of the normal modes.

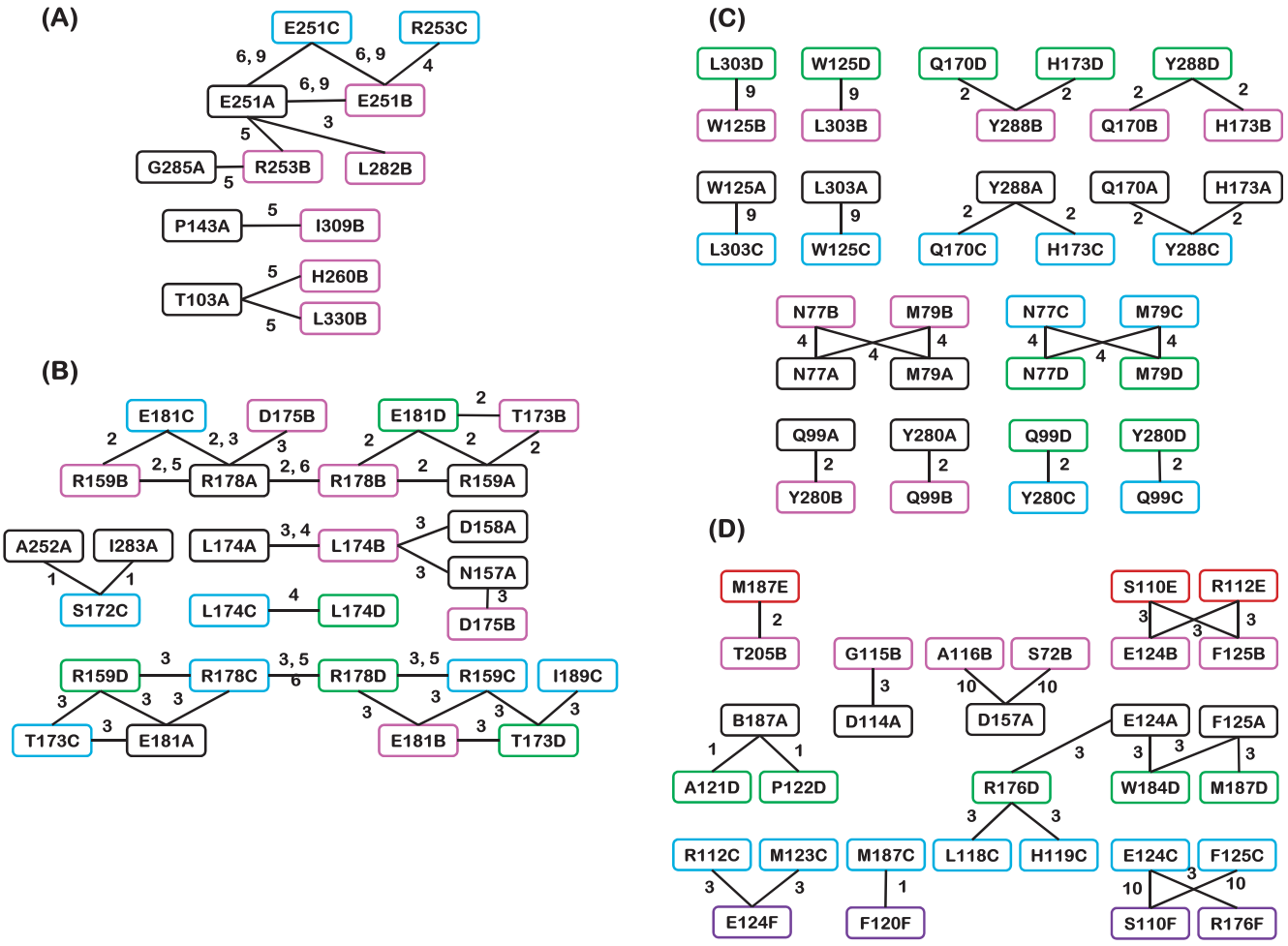

Figure 7 Networks of residues with high BTWN on inter-subunit interfaces. In each box, an amino acid name, residue number, and chain name of a residue with high BTWN are presented. The line colors of the boxes (black, red, cyan, green, brown, and violet) indicate the chains A, B, C, D, E, and F, respectively. The two residues are connected if they satisfy the conditions described in the text. The figure on the line indicates a normal mode number in which these conditions are satisfied. These residues are also shown on the 3D structures in Figure 1.

Their numbers are indicated in Figure 7. The locations of the residues shown in Figures 1 and 7 are not necessarily symmetric because subunits move with phase shifts in a standing-wave-type motion. In particular, asymmetricity is pronounced in the trimer, AcNiR.

In Figure 1, it is apparent that the residues shown in Figure 7 connect the neighboring subunits. The amino acid pairs that draw our attention in Figure 7 are salt bridge pairs (R-E and R-D) and hydrophobic residue pairs (L-L, L-W, Y-Q, Y-H, M-M, and F-M). It is well established that such amino acid pairs are frequently observed in the statistical data on the inter-subunit interfaces of oligomers [41]. This indicates the importance of hydrogen bonding and of the electro static and hydrophobic interactions between residues. However, it should be noted that Figure 7 specifies residue pairs that may be potentially important on the inter-subunit interfaces from a dynamical perspective.

Discussion

In the present study, we confined ourselves to characterizing the motions of the lowest-frequency normal modes, whereas time-averaged properties have been discussed in most of the NMA studies. For example, the time-averaged fluctuations of atoms provide information only about the extent to which the local structures fluctuate and not regarding what type of motion they undergo, i.e., translation, rotation, stretching, etc. The time-averaged cross-correlation between the motions of atoms provides the following information: if it is near one, the two atoms move in the same direction; if it is near zero, they move in various directions in the different normal modes; if it is near minus one, they move in opposite directions. However, in the final case, they do not provide directional information about mutual motions of domains and subunits such as sliding and approaching/separating motions. Such directional information about the motions is essential for understanding ligand-induced conformational variations in proteins and can be derived only from the motions of the lowest-frequency normal modes rather than time-averaged properties.

Figure 3 shows a variety of motions of subunits in the oligomer depending on the normal modes. However, the diverse motions can be comprehensively distinguished by the radial, tangential, and z-axis components in the cylindrical coordinate system. In addition, it is a convenient method for imaging the subunit motions. If this method is applied to many oligomers, it may be feasible to classify the motions of oligomers.

We examined one trimer, two tetramers, and one hexamer in this study. We had already studied the inter-subunit interface of dimers [39]. We were interested in oligomers with over two subunits because they were expected to have significantly different features from dimers. For example, they can be organized in a ring form or in a closed-packed form. The subunits interact with more than one subunit. Consequently, their inter-subunit interface areas grow significantly wider than dimers. We paid special attention to the residues on the inter-subunit interface as we were interested in whether or not the difference between the residues on the inter-subunit interface and non-interface ones is reduced as the number of subunits increases. Contrary to our expectation, the residues on the inter-subunit interface move so as to retain the conformation of the subunits. This indicates that the intrinsic motions of individual subunits mainly determine the oligomer dynamics and that the interactions between subunits manifest as perturbation on it.

Meanwhile, the arrangements of subunits, such as a ring form and a closed-packed form, regulate the oligomer dynamics significantly. The symmetrical and standing-wave type motions are evident in the cylindrical coordinate system. These motions can be observed only in the oligomers with over two subunits.

The dynamic PSNs were also investigated to characterize the motions of the lowest-frequency normal modes. PSNs are generally defined for a static structure and occasionally for a dynamic structure by using time-averaged cross-correlation between atomic motions. However, in our experience, the time-averaged cross-correlations are strongly affected by contact/non-contact of the residues. As a result, the difference between the static and dynamic PSNs is not significant. Meanwhile, the dynamic PSNs based on the lowest-frequency normal modes have certain unique features depending on the normal modes.

The PSN method has been demonstrated to be effective for detecting both important residues for protein function (such as an active site residue) and communication pathways between remote residues that undergo their allosteric conformational modifications. Figure 5 shows that certain residues binding to an auxiliary small molecule have high BTWN. This indicates their importance in the dynamic structure of the oligomer. It should be also noted that the residues on a few of the domain boundaries have high BTWN in certain normal modes in the dynamic PSN.

In this study, we paid attention to the residues on the inter-subunit surface. They were examined using one of the centrality measures, BTWN (betweenness), as in other studies. In our dynamic PSN, residues are connected if they are in contact and move coherently. Consequently, a residue with higher BTWN would have higher control over the mutual motions of neighboring subunits. This is because many residues in the different subunits communicate with each other while passing through that residue. The pair of residues from different subunits that are in contact on the inter-subunit interface and have high BTWN are observed as shown in Figures 1 and 7. It is indicated that they may play an important role in the oligomer dynamics.

The cluster of residues with high BTWN shown in Figure 7 can be extended to non-interface residues. Larger networks exist that include both inter-subunit interface and non-interface residues with high BTWN. In such networks, a few

active site and molecule binding site residues are linked to the non-interface residue in the interior. The analysis of such networks may provide a deep insight into the oligomer dynamics. However, because more complex analysis is required, these studies will be undertaken in future work.

Acknowledgement

This paper is dedicated to Professor Nobuhiro Gō on the occasion of his 80th birthday. This work was supported by a JSPS Grant-in-Aid for Scientific Research (C) (grant no. 16K00407).

Conflicts of Interest

H. W. and S. E. declare that they have no conflict of interest.

Author Contribution

H. W. and S. E. directed the entire project and co-wrote the manuscript.

References

[1] Goodsell, D. S. & Olson, A. J. Structural symmetry and protein function. *Annu. Rev. Biophys. Biomol. Struct.* **29**, 105–153 (2000).
[2] Seno, Y. & Gō, N. Deoxymyoglobin studied by the conformational normal mode analysis: I. Dynamics of globin and the heme-globin interaction. *J. Mol. Biol.* **216**, 95–109 (1990).
[3] Seno, Y. & Gō, N. Deoxymyoglobin studied by the conformational normal mode analysis: II. The conformational change upon oxygenation. *J. Mol. Biol.* **216**, 111–126 (1990).
[4] Bahar, I., Lezon, T. R., Bakan, A. & Shrivastava, I. H. Normal mode analysis of biomolecular structures: functional mechanisms of membrane proteins. *Chem. Rev.* **110**, 1463–1497 (2010).
[5] Ishida, H., Jochi, Y. & Kidera, A. Dynamic structure of subtilisin-eglin c complex studied by normal mode analysis. *Proteins* **32**, 324–333 (1998).
[6] Niv, M. Y. & Filizola, M. Influence of oligomerization on the dynamics of G-protein coupled receptors as assessed by normal mode analysis. *Proteins* **71**, 575–586 (2008).
[7] Marcos, E., Crehuet, R. & Bahar, I. Changes in dynamics upon oligomerization regulate substrate binding and allostery in amino acid kinase family members. *PLoS Comput. Biol.* **7**, e1002201 (2011).
[8] Wako, H. & Endo, S. ProMode-Oligomer: database of normal mode analysis in dihedral angle space for a full-atom system of oligomeric proteins. *Open Bioinform. J.* **6**, 9–19 (2012).
[9] Matsunaga, Y., Koike, R., Ota, M., Tame, J. R. H. & Kidera, A. Influence of structural symmetry on protein dynamics. *PLoS One* **7**, e50011 (2012).
[10] Wako, H., Kato, M. & Endo, S. ProMode: a database of normal mode analyses on protein molecules with a full-atom model. *Bioinformatics* **20**, 2035–2043 (2004).
[11] Wako, H. & Endo, S. Normal mode analysis based on an elastic network model for biomolecules in the Protein Data Bank, which uses dihedral angles as independent variables. *Comput. Biol. Chem.* **44**, 22–30 (2013).
[12] Wako, H., Endo, S., Nagayama, K., & Gō, N. FEDER/2: program for static and dynamic conformational energy analysis of macro-molecules in dihedral angle space. *Comput. Phys. Comm.* **91**, 233–251 (1995).
[13] Noguti, T. & Gō, N. Dynamics of native globular proteins in terms of dihedral angles. *J. Physical Soc. Japan* **52**, 3283–3288 (1983).
[14] Noguti, T. & Gō, N. A method of rapid calculation of a second derivative matrix of conformational energy for large molecules. *J. Physical Soc. Japan* **52**, 3685–3690 (1983).
[15] Abe, H., Braun, W., Noguti, T. & Gō, N. Rapid calculation of first and second derivatives of conformational energy with respect to dihedral angles for proteins general recurrent equations. *Comput. Chem.* **8**, 239–247 (1984).
[16] Wako, H. & Gō, N. Algorithm for rapid calculation of Hessian of conformational energy function of proteins by supercomputer. *J. Comput. Chem.* **8**, 625–635 (1987).
[17] Higo, J., Seno, Y. & Gō, N. Formulation of static and dynamic conformational energy analysis of biopolymer systems consisting of 2 or more molecules—Avoiding a singularity in the previous method. *J. Physical Soc. Japan* **54**, 4053–4058 (1985).
[18] Wako, H. & Endo, S. Normal mode analysis as a method to derive protein dynamics information from the Protein Data Bank. *Biophys. Rev.* **9**, 877–893 (2017).
[19] Tirion, M. M. Large amplitude elastic motions in proteins from a single-parameter, atomic analysis. *Phys. Rev. Lett.* **77**, 1905–1908 (1996).
[20] Dobbins, S. E., Lesk, V. I. & Sternberg, M. J. Insights into protein flexibility: The relationship between normal modes and conformational change upon protein-protein docking. *Proc. Natl. Acad. Sci. USA* **105**, 10390–10395 (2008).
[21] Tama, F. & Sanejouand, Y. H. Conformational change of proteins arising from normal mode calculations. *Protein Eng. Des. Sel.* **14**, 1–6 (2001).
[22] Wako, H. & Endo, S. Ligand-induced conformational change of a protein reproduced by a linear combination of displacement vectors obtained from normal mode analysis. *Biophy. Chem.* **159**, 257–266 (2011).
[23] Amitai, G., Shemesh, A., Sitbon, E., Shklar, M., Netanely, D., Venger, I., *et al.* Network analysis of protein structures identifies functional residues. *J. Mol. Biol.* **344**, 1135–1146 (2004).
[24] Sethi, A., Eargle, J., Black, A. A. & Luthey-Schulten, Z. Dynamical networks in tRNA: protein complexes. *Proc. Natl. Acad. Sci. USA* **106**, 6620–6625 (2009).
[25] Raimondi, F., Felline, A., Seeber, M., Mariani, S. & Fanelli, F. A mixed protein structure network and elastic network model approach to predict the structural communication in biomolecular systems: The PDZ2 domain from tyrosine phosphatase 1E as a case study. *J. Chem. Theory Comput.* **9**, 2504–2518 (2013).
[26] Tse, A. & Verkhivker, G. M. Molecular dynamics simulations and structural network analysis of c-Abl and c-Src kinase core proteins: Capturing allosteric mechanisms and communication pathways from residue centrality. *J. Chem. Inf. Model.* **55**, 1645–1662 (2015).
[27] Brysbaert, G., Mauri, T., de Ruyck, J. & Lensink, M. F. Identification of key residues in proteins through centrality analysis and flexibility prediction with RINspector. *Curr. Protoc. Bioinformatics* **65**, e66 (2019).
[28] Gasper, P. M., Fuglestad, B., Komives, E. A., Markwick, P. R. & McCammon, J. A. Allosteric networks in thrombin distinguish procoagulant vs. anticoagulant activities. *Proc. Natl. Acad. Sci. USA* **109**, 21216–21222 (2012).
[29] Skjærven, L., Yao, X. Q., Scarabelli, G. & Grant, B. J. Integrating protein structural dynamics and evolutionary analysis with Bio3D. *BMC Bioinformatics* **15**, 399 (2014).

[30] Seeber, M., Felline, A., Raimondi, F., Mariani, S. & Fanelli, F. WebPSN: a web server for high-throughput investigation of structural communication in biomacromolecules. *Bioinformatics* **31**, 779–781 (2015).
[31] Blakeley, M. P., Hasnain, S. S. & Antonyuk, S. V. Sub-atomic resolution X-ray crystallography and neutron crystallography: promise, challenges and potential. *IUCrJ.* **2**, 464–474 (2015).
[32] Lubkowski, J., Dauter, M., Aghaiypour, K., Wlodawer, A. & Dauter, Z. Atomic resolution structure of *Erwinia chrysanthemi* L-asparaginase. *Acta Crystallogr. D Biol. Crystrallogr.* **D59**, 84–92 (2003).
[33] Safonova, T. N., Mikhailov, S. N., Veiko, V. P., Mordkovich, N. N., Manuvera, V. A., Alekseev, C. S., *et al.* High-*syn* conformation of uridine and asymmetry of the hexameric molecule revealed in the high-resolution structures of *Shewanella oneidensis* MR-1 uridine phosphorylase in the free form and in complex with uridine. *Acta Crystallogr. D Biol. Crystrallogr.* **D70**, 3310–3319 (2014).
[34] Maguid, S., Fernandez-Alberti, S. & Echave, J. Evolutionary conservation of protein vibrational dynamics. *Gene* **422**, 7–13 (2008).
[35] Liu, Y. & Bahar, I. Sequence evolution correlates with structural dynamics. *Mol. Biol. Evol.* **29**, 2253–2263 (2012).
[36] Echave, J. Why are the low-energy protein normal modes evolutionarily conserved? *Pure Appl. Chem.* **84**, 1931–1937 (2012).
[37] Celniker, G., Nimrod, G., Ashkenazy, H., Glaser, F., Martz, E., Mayrose, I., *et al.* ConSurf: using evolutionary data to raise testable hypotheses about protein function. *Isr. J. Chem.* **53**, 199–206 (2013).
[38] Laskowski, R. A., Jabłońska, J., Pravda, L., Vařeková, R. S. & Thornton, J. M. PDBsum: Structural summaries of PDB entries. *Protein Sci.* **27**, 129–134 (2018).
[39] Tsuchiya, Y., Kinoshita, K., Endo, S. & Wako, H. Dynamic features of homodimer interfaces calculated by normal-mode analysis. *Protein Sci.* **21**, 1503–1513 (2012).
[40] Kinjo, A. R., Bekker, G.-J., Wako, H., Endo, S., Tsuchiya, Y., Sato, H., *et al.* New tools and functions in data-out activities at Protein Data Bank Japan (PDBj). *Protein Sci.* **27**, 95–102 (2018).
[41] Brinda, K. V. & Vishveshwara, S. Oligomeric protein structure networks: insights into protein-protein interactions. *BMC Bioinformatics* **6**, 296 (2005).